

## SPECTROSCOPIC INVESTIGATIONS OF PIGMENTS ON A LATE ROMAN MILESTONE FROM CALABRIA, SOUTHERN ITALY

*Francesco Caridi\**, *Barbara Testagrossa\*\**, *Pasquale Faenza\*\*\**, *Giuseppe Aciri\*\**

\* Environmental Protection Agency of Calabria (ArpaCal) – Department of Reggio Calabria, Reggio Calabria, Italy

\*\* University of Messina, Department BIOMORF, Messina, Italy

\*\*\* G. Rohlfs Museum, Bova Marina (RC), Italy

### Abstract

In this paper the compositional and structural analysis of a Roman milestone, preserved in the Antiquarium of the archaeological park of Bova Marina, Reggio Calabria, south of Italy, was performed. A combination of spectroscopic techniques was employed for this purpose. Scanning Electron Microscopy with Energy Dispersive X-ray spectroscopy (SEM+EDX) was used for the morphological investigation and quantitative elemental analysis of the investigated samples; Raman Spectroscopy (RS) was employed to identify their crystalline mineral components and to study their microstructure. The chemical analysis allowed us to identify elements and compounds, closely related to the sample preparation, with the aim to investigate about nature and the possible artistic technique, to better understand the original aspect of this late-Empire road system.

### Keywords

Scanning Electron Microscopy with Energy Dispersive X-ray spectroscopy; Raman Spectroscopy; Roman milestone; Late-Empire road system

### 1. Introduction

The compositional analysis of ancient cultural heritages, by using spectroscopic techniques, represents an important aspect of the new archaeological researches, because it is an essential tool for the knowledge of ancient artifacts fabrication technology (Torrise, et al., 2009).

Many analytical techniques can be used for these purposes, including conventional, neutron-based, high energy X-ray-based and imaging techniques (Rant, et al., 2006; Fukunaga & Hosako, 2010; Caridi, Mezzasalma, & Castrizio, 2014). Recently, different mass spectrometric ones have been exploited in this field for surface analysis, such as the inductively coupled plasma-mass spectrometry (ICP-MS), the Rutherford backscattering spectroscopy (RBS) and the nuclear reaction analysis, which are very useful for many archaeometrical applications (Caridi, et al., 2016; Caridi, Marguccio, D'Agostino, Belvedere, & Belmusto, 2016; Mandò, Fedi, & Grassi, 2011).

In the present article Scanning Electron Microscopy with Energy Dispersive X-ray

(SEM+EDX) and Raman Spectroscopy (RS) were employed, because they represent two of the most versatile methods and they are widely applied to samples of archaeological interest (Torrise, et al., 2010; Caridi, Sabatino, Mezzasalma, Faenza, & Castrizio, 2014; Liritzis, Zacharias, Papageorgiou, Tsaroucha, & Palamara, 2018; Aciri, Testagrossa, Faenza, & Caridi, 2020).

Experimental measurements were performed in order to analyze the chemical composition, to identify the crystalline mineral components and to study the microstructure of powdered samples from the upper (A) and the lower (B) parts of a Roman milestone, now preserved in the Antiquarium of the archeological park of Bova Marina, Reggio Calabria, south of Italy (Coppola, 2009).

Samples were taken, during restoration works, from the two inscriptions on the ends of the miliary, engraved in a contrasting way at different times during the fourth century AD. The oldest of the inscriptions (part B) *Imp(erator) Caes(ar) M(arcus) Au(relius) / Val(erius) Maxentius / p(ius) f(elix), invictus / ac perpetuus / semper Aug(ustus) / b(ono) r(ei) p(ublicae) n(atatus)* certifies that the

312 AD). The second (part A), however, was engraved between 364 and 367 AD, when the stone was reused upside down to honor the emperors Valentinian and Valens, whose names are now legible in the upper part, *Dd. nn (i.e. dominis nostri duobus) / invictissimis / imperatoribus / Valentinian / ac Valenti/Aagg. (i.e. Augusti duobus) bono / (ei) p(ublicae) natis.*

The artifact represents a rare testimony of the road layout that connected Reggio Calabria to Taranto (south of Italy) in the late ancient period (Miller, 1916; Faenza, 2009), roughly following the progress of the current Italian SS106 road, with the exception of the sections falling towards the interior of the foothills, indispensable to cross the promontories that lapped the coasts.

This milestone was in fact found near Capo San Giovanni d'Avalos, not far from the archaeological area, identified in the Roman parking station of *Skile statio* reported both in the *Tabula Peutingeriana* and in two other later *itineraria* (Costamagna, 1991).

The absence, in the two inscriptions, of the distance from *Regium* and of any reference to a

road maintenance intervention, places this milestone in the type of stones often used in the 4<sup>th</sup> century AD as political propaganda tools (Grelle & Volpe, 1996; Buonopane, 2003); in fact, it is different from the two road markers, built at the time of Licinius and Constantine, found in 1774 in Melito di Porto Salvo (south of Italy), relating respectively to the XX and XXI miles from *Regium* (Costabile, 1987). These distances have made it possible to identify the location of the *Decastadium statio*, as indicated by the *itinerarium Antoninii* twenty miles from *Regium* (Costabile, 1987). However, this last source, the oldest one that has come down to us (3<sup>rd</sup> century AD), does not report, following the *Decastadium statio*, that of *Skile*.

This suggests that the latter parking station arose at a later time, or that the route reported by the *itinerarium Antoninii* refers to a road route different from that indicated in the later road maps, starting with the *Tabula Peutingeriana*, a medieval copy of an original of the III-IV century AD (Coppola, 2009; Prontera, 2003; Talbert, 2010).

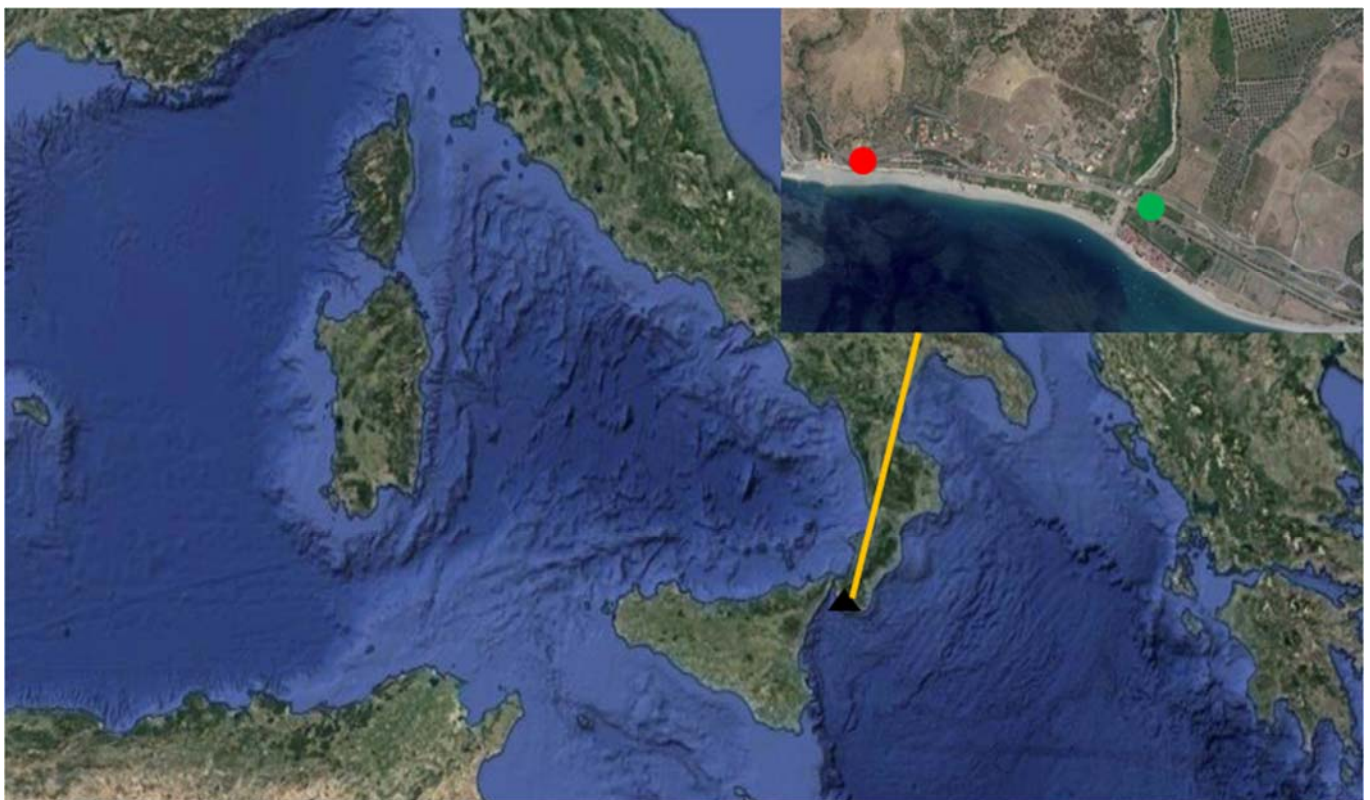


**Fig. 1:** Map of the geographical area, in the south of Italy, where the milestone was found (triangle symbol). In the upper right corner are highlighted the location of discovery (red circle) and the Antiquarium of the archaeological park of Bova Marina (green circle) where the milestone is preserved.

## 2. Materials and Methods

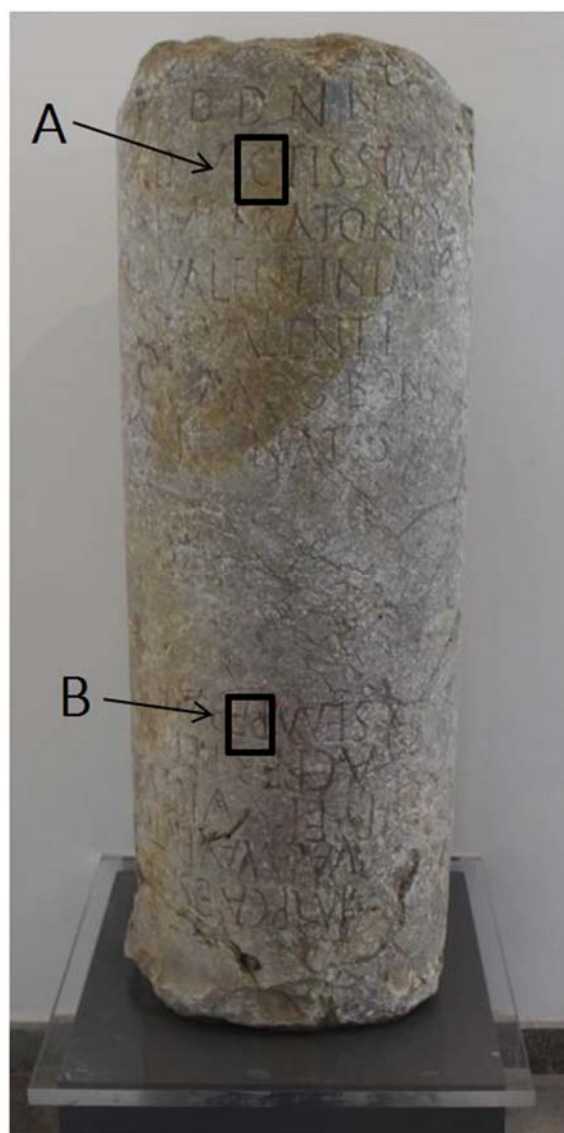
Figure 1 reports the geographical area in the south of Italy where the milestone was found (triangle symbol). A modern map appears on the top right box of Figure 1. Red and green circles in the map indicate the location where the Roman milestone was found (DMS geographical coordinates  $37^{\circ} 55' 31.523''$  N,  $15^{\circ} 56' 16.321''$  E) and where the milestone is preserved now (DMS geographical coordinates  $37^{\circ} 55' 26.832''$  N,  $15^{\circ} 57' 5.335''$  E) respectively.

Figure 2 shows the investigated milestone (Inventory No: C57 - Archeology, Fine Arts and Landscape for the metropolitan city of Reggio Calabria and the province of Vibo Valentia). Two areas, A and B, are highlighted in Figure 2. They correspond to the upper (A) and the lower (B) parts of the Roman milestone. Powders were taken, during restoration works, from A and B areas and analyzed by SEM+EDX and RS. Both techniques do not require sample preparation and are not destructive.

### 2.1 SEM+EDX

Samples (powdered particles) were analyzed by Scanning Electron Microscope (SEM) (Jeol JMC-6000) to evaluate their morphological characteristics (Jeol, 2019). They were mounted on adhesive black carbon tabs, pre-mounted on the sample holder. Samples surface was scanned using an electron beam, generated by an electron gun, in X-Y directions. By the scanning of an incident electron beam on the sample, secondary electrons (SE) and backscattered electrons (BE) were emitted from the sample surface. SE and BE were detected as a signal and the morphology of the sample surface was converted in a 3D image on the monitor display. The SEM measurements were conducted at 15 kV and a magnification of X100 was used.

Elemental analysis of powdered particles was performed by the Energy Dispersive X-Ray analyzer (EDX) Jeol DX200s. As a result, an X ray spectrum was obtained and the elements in the sample were identified from the peak energy and quantitatively analyzed from the quantity of the peaks. The analysis results were obtained by referring to a reference energy spectrum of calibration included in the instrument library. The qualitative and quantitative elemental analysis were performed at different points of the surface of each powdered sample and the obtained



**Fig. 2:** Photo of the Roman milestone, with the provenience area of the investigated samples put in evidence

results are related to the mean value of the measurements.

### 2.2 Raman Spectroscopy

Raman measurements of the powdered samples were performed by using a Thermo Fisher Scientific DXR-SmartRaman Spectrometer (Thermo Fisher Scientific, 2019).

The experimental set-up was equipped with 180-degree sampling accessory. The spectra were acquired using a diode laser source with the excitation wavelength of 780 nm. All Raman spectra were acquired over the wavenumber range of  $3400 - 50 \text{ cm}^{-1}$  with a resolution of  $1.9285 \text{ cm}^{-1}$  and irradiated with a laser power of 24 mW, coming out from a  $50 \text{ }\mu\text{m}$  spot.

In order to obtain high signal to noise ratio (S/R), the Raman spectrum of each sample was obtained after collecting 32 sample exposures, and the duration of each exposure during data collection was set equal to 15.0 s. Total acquisition time was 8 minutes for each spectrum. All Raman spectra were stored in .SPA format and the post processing analysis was performed by using the Omnic for dispersive Raman 9.0 software.

### 3. Results and Discussion

Powdered particles were analyzed by SEM+EDX technology.

The obtained morphological and elemental results are reported in Figure 3 and in Table 1.

The Al ( $K\alpha$ ) contribution was not considered because it was related to the sample holder. The most abundant element is Pb in both samples; presence of traces of Mn, Cu and Mg were also observed, probably due to the impurity in calcium phosphate.

Raman spectra were acquired for each sample, in order to identify materials and pigments present in the investigated dust (Gutman, Zanier, Lux, & Kramar, 2016).

Figure 4a reports the Raman spectrum of the sample A. It shows the typical fingerprint of red lead, also called minium ( $Pb_3O_4$ ), responsible for the orange coloration, with distinguishable bands at 52, 62, 80, 118, 146, 224, 310, 384, 458, 475, 541  $cm^{-1}$ . The major bands of the spectrum are at 118  $cm^{-1}$ , which corresponds to the bending vibrations of deformation of the angle O-Pb<sup>IV</sup>-O, and at 542  $cm^{-1}$  which corresponds to the stretching vibrations of the Pb<sup>IV</sup>-O bond. A band located at 1051  $cm^{-1}$  also appears, related to the stretching vibrations of ( $CO_3^{2-}$ ) and indicating the presence of lead carbonate.

The absence of the weak band located at 828  $cm^{-1}$ , could allow to distinguish between cerussite ( $PbCO_3$ ) and hydrocerussite ( $PbCO_3 \cdot Pb(OH)_2$ ), since this band is ascribed to the hydrated lead carbonate. Two broad bands located at 1318 and

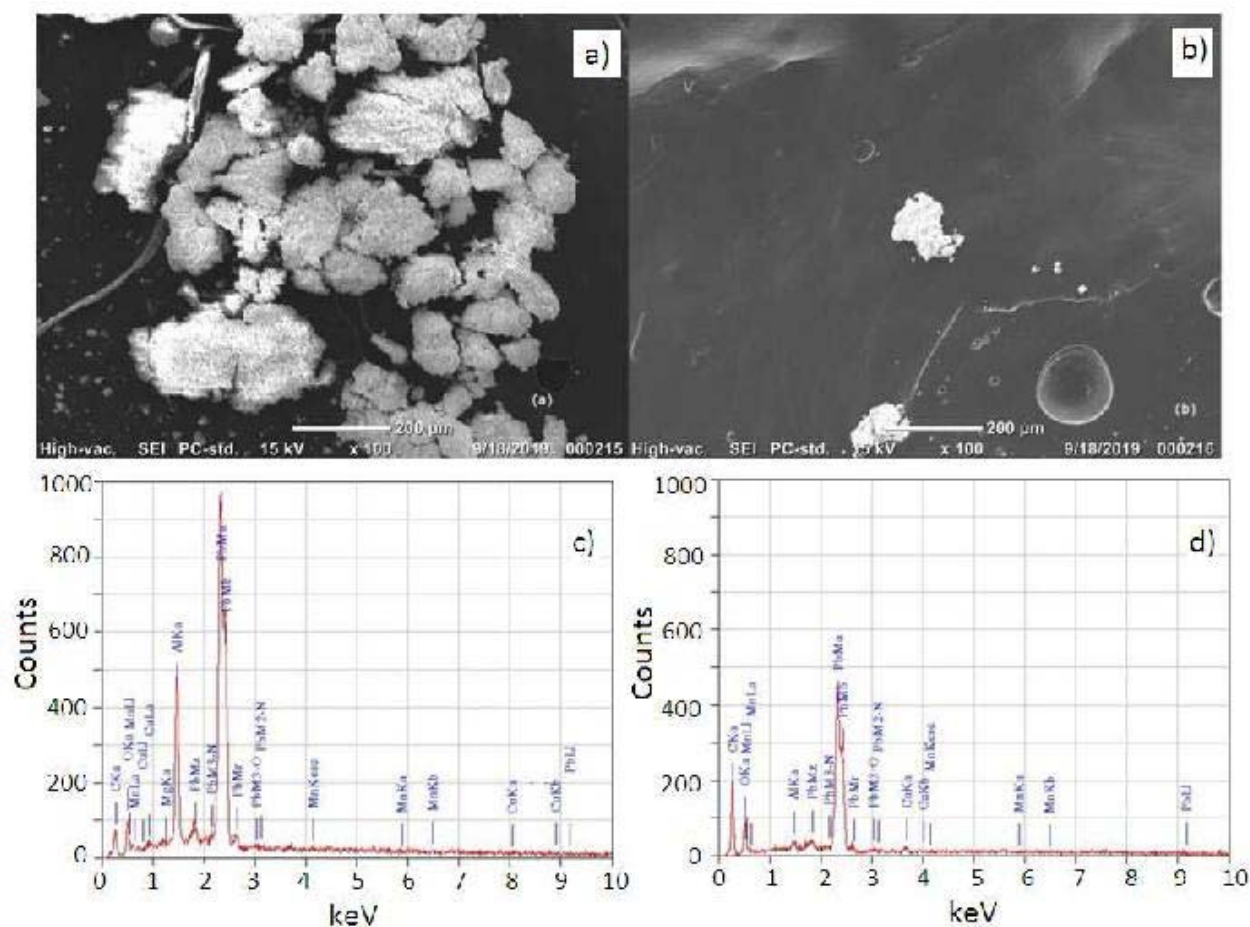


Fig. 3: SEM images and EDX elemental analysis of samples A (a, c) and B (b, d).

**Tab. 1:** SEM+EDX evaluations (mean percentage  $\pm$  standard deviation).

Element	Sample A	Sample B	
		Element	%
C	3.68 $\pm$ 0.18	C	16.81 $\pm$ 0.84
O	4.13 $\pm$ 0.21	O	8.45 $\pm$ 0.42
Mn	1.77 $\pm$ 0.09	Mn	2.33 $\pm$ 0.12
CuL( $\alpha$ )	1.52 $\pm$ 0.08	CuL( $\alpha$ )	-----
CuL( $\beta$ )	1.72 $\pm$ 0.09	CuL( $\beta$ )	-----
Mg $\kappa\alpha$	1.52 $\pm$ 0.08	Mg $\kappa\alpha$	-----
PbM $\zeta$	4.81 $\pm$ 0.24	PbM $\zeta$	2.93 $\pm$ 0.15
PbM3-N	2.95 $\pm$ 0.15	PbM3-N	1.64 $\pm$ 0.08
Pb M $\alpha$	45.40 $\pm$ 2.27	Pb M $\alpha$	39.05 $\pm$ 1.95
Pb M $\beta$	27.03 $\pm$ 1.35	Pb M $\beta$	22.84 $\pm$ 1.14
Pb-M $\rho$	2.70 $\pm$ 0.13	Pb-M $\rho$	1.29 $\pm$ 0.06
Pb-M3-O	1.33 $\pm$ 0.07	Pb-M3-O	0.86 $\pm$ 0.04
Pb-M2-N	1.42 $\pm$ 0.07	Pb-M2-N	0.86 $\pm$ 0.04
		Ca $\kappa\alpha$	1.98 $\pm$ 0.10
		Ca $\kappa\beta$	0.95 $\pm$ 0.05

1573  $\text{cm}^{-1}$  indicate the presence of carbonaceous material. The absence of the  $\nu(\text{CH})$  modes near 3000  $\text{cm}^{-1}$ , indicates that this is probably amorphous carbon and not a colored resin.

Figure 4b reports the Raman spectrum of the sample B. It shows an intense peak located at 134  $\text{cm}^{-1}$  and a band centered at 270  $\text{cm}^{-1}$ . These Raman bands closely correspond to massicot, which is orthorhombic lead monoxide (PbO), possibly with a contribution from litharge, which is tetragonal PbO. Also, in the sample B two broad bands, centered at 1303 and 1590  $\text{cm}^{-1}$ , are present due to the possible presence of amorphous carbon.

The peak located at 1084  $\text{cm}^{-1}$  is characteristic of the presence of calcite.

All pigments were identified by comparison of the obtained Raman peaks with those in standard pigment databases (Caggiani, Cosentino, & Mangone, 2016; Marucci, Beeby, Parker, & Nicholson, 2018).

Obtained experimental results confirm that the registration carried out on the milestone between 307 and 313 AD was colored using massicot, a pigment obtained from the Romans from direct oxidation of the white lead at 300  $^{\circ}\text{C}$ .

The presence also of calcite allows us to suppose that the massicot was spread on a preparatory layer. This expedient, also found in other milestones found in northern Italy, in France and in Jordan (Basso, 2018; Graf, 1999), was not detected in the subsequent epigraph, colored between 364 and 367 AD using exclusively the

minium, a pigment widespread in Roman times and also obtained by heating the lead, but at higher temperatures than massicot. The absence of a preparatory layer is completely in line with the scarce attention paid to the execution of the milestones in the second half of the fourth century A.D., compared to previous periods.

However, what is important to note is the presence on both inscriptions of pigments derived from the heating of lead.

Their use during a limited time between 306 AD and 367 AD, could be found, in the absence of other milestones of late ancient Calabria bearing traces of pigment, a fundamental clue to understand the diffusion of lead reds in the coloring of this kind of artifacts.

About the presence of amorphous carbon in samples A and B, there is no doubt that it can be related to the use of a graphite tip used to facilitate the reading of the epigraphs in the aftermath of the discovery of the find (1913 AD), still today visible along the edge of some letters relevant to both inscriptions.

#### 4. Conclusions

The aim of this work was to investigate about painting techniques and pigments used in the inscriptions of the Roman milestone of Bova Marina, which we know engraved in the fourth century AD, about sixty years apart: the oldest during the Maxentius age (307-312 AD) and the other one between 364 AD and 367 AD.

To perform this study two different analysis were conducted: SEM+EDX and Raman measurements. The first one provides morphological and chemical identification, while Raman measurements give information about the characteristic vibration levels of each constituent.

Obtained experimental results confirm that the registration carried out on the milestone between 307 and 313 AD. (sample B) was colored using massicot, and the presence of calcite was due to the massicot spread on a preparatory layer. This expedient was not detected in the subsequent epigraph (sample A), colored between 364 and 367 AD using exclusively the minium.

Obtained experimental results uniquely characterize, for the first time, this kind of cultural heritage from the point of view of the pigments and techniques used for making the engravings; due to the lack of knowledge regarding traces of colors conserved on late ancient milestones, we plan to extend the study to other Roman milestones in the next future, to characterize this type of finds and thus confirm the experimental evidence of the artistic technique.<sup>1</sup>

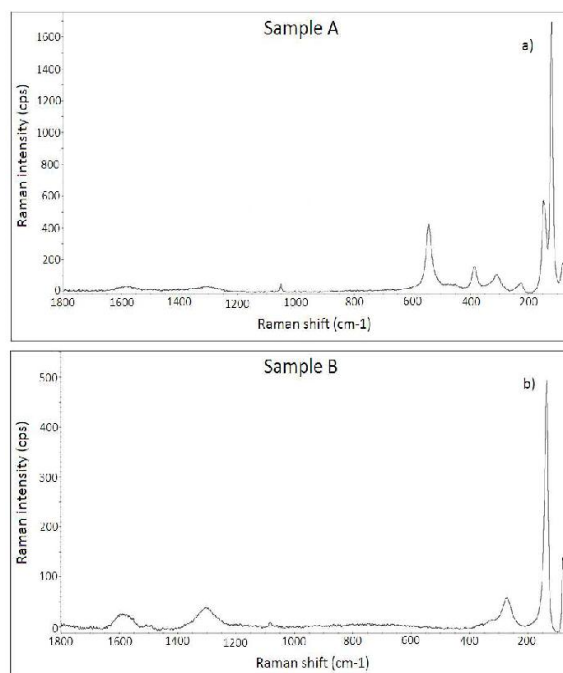


Fig. 4: The Raman spectrum of samples A (a) and B (b).

<sup>1</sup>. The authorship of the paper should be attributed as follows: Francesco Caridi: Conceptualization, Investigation, Writing original draft preparation; Barbara Testagrossa: Formal

Analysis, Data Curation; Pasquale Faenza: Conceptualization, Resources; Giuseppe Acri: Formal Analysis, Data Curation, Writing original draft preparation.

## REFERENCES

- Acri, G., Testagrossa, B., Faenza, P., & Caridi, F. (2020). Spectroscopic analysis of ancient gilts of the Antonello Gagini Annunciation's sculptural group, church of the St. Theodore Martyr in Bagaladi, Reggio Calabria, Italy. *Mediterranean Archaeology and Archaeometry*, 20(1). doi:10.5281/zenodo.336481
- Basso, P. (2018). Cosa Raccontano i cippi miliari. *Quaderni friulani di archeologia*, Anno XXVIII, 107-122.
- Buonopane, A. (2003). Abusi epigrafici tardo-antichi: i miliari dell'Italia settentrionale (regiones X e XI). *Usi ed abusi epigrafici. Atti del Colloquio Internazionale di epigrafi a latina*. (pp. 343-354). Roma: M.G. Angeli Bertinelli e A. Donati.
- Caggiani, M. C., Cosentino, A., & Mangone, A. (2016). Pigment Checker 3.0, a handy set for conservation scientists: A free online Raman spectra database. *Microchemical Journal*, 129, 123-132. doi:10.1016/j.microc.2016.06.020
- Caridi, F., D'Agostino, M., Marguccio, S., Belvedere, A., Belmusto, G., Marcianò, G., Sabatino, G., & Mottese, A. (2016). Radioactivity, granulometric and elemental analysis of river sediments samples from the coast of Calabria, south of Italy. *European Physical Journal Plus*, 131(5), 136.
- Caridi, F., Marguccio, S., D'Agostino, M., Belvedere, A., & Belmusto, G. (2016). Natural radioactivity and metal contamination of river sediments in the Calabria region, south of Italy. *European Physical Journal Plus*, 131(5), 155.
- Caridi, F., Mezzasalma, A. M., & Castrizio, E. D. (2014). An investigation on the patina of ancient bronze coins. *Radiation Effects and Defects in Solids*, 169(5), 371-379.
- Caridi, F., Sabatino, G., Mezzasalma, A. M., Faenza, P., & Castrizio, E. D. (2014). Spectroscopic analyses of an ancient silver fragment of the reliquary bust of St. Leo. *Radiation Effects and Defects in Solids*, 169(7), 573-583.
- Coppola, G. (2009). La viabilità in età romana tra Regium e Bova Marina. In *Il Parco Archeologico Deri-San Pasquale. Bova Marina* (pp. 43-48). Reggio Calabria: Agostino, R.
- Costabile, F. (1987). Due miliari da Decastadium (Bruttii) e la damnatio memoriae di Licinio e Liciniano. In *Hestiasis. Studi di tarda antichità offerti a Salvatore Calderone, III* (pp. 219-234.). Messina: G. Puglisi.
- Costamagna, L. (1991). La sinagoga di Bova Marina nel quadro degli insediamenti tardoantichi della costa Ionica meridionale della Calabria. *Mélanges de l'École française de Rome. Moyen-Age*, 103(2), 611-630. doi:10.3406/mefr.1991.3190
- Faenza, P. (2009). *Bova Marina. Storia arte e natura nella Calabria Greca*. Reggio Calabria: Iiriti.
- Fukunaga, K., & Hosako, I. (2010). Innovative non-invasive analysis techniques for cultural heritage using terahertz technology. *Comptes Rendus Physique*, 11(7-8), 519-526. doi:10.1016/j.crhy.2010.05.004
- Graf, D. F. (1999). The Via Nova Traiana in Arabia Petraea. In J. H. Humphrey (Ed.), *The Roman and Byzantine Near East: some recent archaeological research* (Vol. 2, pp. 241-265). Portsmouth, RI, USA: Journal of Roman Archaeology.
- Grelle, F., & Volpe, G. (1996). Aspetti della geografia amministrativa ed economica della Calabria in età tardo antica. In M. Pani (Ed.), *Epigrafia e territorio politica e società. Temi di antichità Romane* (Vol. 4, pp. 113-155.). Bari: Edipuglia.

Gutman, M., Zanier, K., Lux, J., & Kramar, S. (2016). Pigment analysis of roman wall paintings from two villae rusticae in Slovenia. *Mediterranean Archaeology and Archaeometry*, 16(3), 193-206. doi:10.5281/zenodo.160970

Jeol. (2019). JMC 6000 User Manual.

Liritzis, I., Zacharias, N., Papageorgiou, I., Tsaroucha, A., & Palamara, E. (2018). Characterisation and analyses of museum objects using pXRF: An application from the Delphi Museum, Greece. *Studia Antiqua et Archaeologica*, 24(1), 31-50.

Mandò, P. A., Fedi, M. E., & Grassi, N. (2011). The present role of small particle accelerators for the study of cultural heritage. *European Physical Journal Plus*, 126(4), 41-50. doi:10.1140/epjp/i2011-11041-9

Marucci, G., Beeby, A., Parker, A. W., & Nicholson, C. E. (2018). Raman Spectroscopic Library Of Medieval Pigments Collected With Five Different Wavelengths For Investigation Of Illuminated Manuscripts. *Analytical Methods*, 10, 1219-1236. doi:10.1039/c8ay00016f

Miller, K. (1916). *Die Peutingersche Tafel oder weltkarte des Castorius*. Stuttgart: Strecker und Schröder.

Prontera, F. (2003). *Tabula Peutingeriana: le antiche vie del mondo*. Firenze: Leo S. Olschki.

Rant, J., Milic, Z., Istenic, J., Knific, T., Lengar, I., & Rant, A. (2006). Neutron radiography examination of objects belonging to the cultural heritage. *Applied Radiation and Isotopes*, 64, 7-12.

Talbert, R. J. (2010). *Rome's world: the Peutinger map reconsidered*. Cambridge: Cambridge University Press.

Thermo Fisher Scientific. (2019). DXR-SmartRaman Spectrometer User Manual.

Torrise, L., Caridi, F., Giuffrida, L., Torrise, A., Mondio, G., Serafino, T., Caltabiano, M., Castrizio, E. D., Paniz, E., & Salici, A. (2010). LAMQS analysis applied to ancient Egyptian bronze coins. *Nuclear Instruments and Methods in Physics Research Section B: Beam Interactions with Materials and Atoms*, 268(10), 1657-1664. doi:10.1016/j.nimb.2010.03.015

Torrise, L., Mondio, G., Mezzasalma, A. M., Margarone, D., Caridi, F., Serafino, T., & Torrise, A. (2009). Laser and electron beams physical analyses applied to the comparison between two silver tetradrachm greek coins. *European Physical Journal D*, 53, 225-232.